Dynamic Response of a Floating Bridge Structure

Thomas Hansen Viuff, Bernt Johan Leira, Ole Øiseth

Norwegian University of Science and Technology, Trondheim, Norway

Xu Xiang

Norwegian Public Roads Administration, Stavanger, Norway

Contact: thomas.h.viuff@ntnu.no

Abstract

A theoretical overview of the stochastic dynamic analysis of a floating bridge structure is presented. Emphasis is on the wave-induced response and the waves on the sea surface are idealized as a zero mean stationary Gaussian process. The first-order wave load processes are derived using linear potential theory and the structural idealization is based on the Finite Element Method. A frequency response calculation is presented for a simplified floating bridge structure example emphasising the influence on von Mises stress in the pontoon from low- and high frequency waves and frequency dependence in hydrodynamic added mass and damping coefficients.

Keywords: Floating bridge; frequency response; linear dynamics; von Mises stress.

1 Introduction

Floating bridges have been around for many thousands of years and throughout the years, they have been used as temporary supply lines or for military purposes. However, it is only during the last three decades or so that floating bridges are being developed to the degree of sophistication, so they can be applied as a critical part of modern infrastructure. Still, compared with land-based bridges, including cable-stayed bridges, limited information [1] is currently available on floating bridges and even less on submerged floating tunnels for transportation. This information is especially true regarding construction records, environmental conditions, durability, operations and performance of the structure.

The limited amount of floating bridges currently in the world is a statement to this fact. Depending on the landscape in the proximity of the floating bridge and on the sea state conditions different types of floating bridges are used. Only three long span floating bridges are currently located in difficult sea state conditions and allows for cars to pass. These are:

i. Hood Canal Bridge (1961) in USA a 2,398 meter long pontoon bridge with a 1,988 meter long anchored floating portion, it is the longest floating bridge in the world located in a saltwater tidal basin, and the third longest floating bridge overall.
ii. Bergsøysund Bridge (1992) in Norway a 931 meter long pontoon bridge with the longest span of 106 meters.
iii. Nordhordland Bridge (1994) in Norway is a combination of a cable-stayed and pontoon bridge. It is the longest free floating bridge without anchorage.

As the rough overview indicates, the theoretical and practical development of floating bridges has been carried out mainly in the USA and in Norway with significant contributions from the industry. In Norway it is mainly the Norwegian University of Science and Technology (NTNU), SINTEF the research organisation and the Norwegian Public Roads Administration (NPRA).

Pioneering studies on floating bridges was carried by Hartz in the 1970's. Around the same time Holan, Sigbjörnsson and Langen carried out similar studies on stochastic dynamics of floating bridges [2] [3] [4] [5]. Later on in 1980 Sigbjörnsson and Langen exemplified the theory using a model of the Salhus floating bridge [6] [7]. In recent years NTNU/SINTEF have led the theoretical evolution within structural mechanics, fluid structure interaction and stochastic modelling of environmental loads applied to the offshore industry in Norway. Many of the same theories can be directly applied in stochastic dynamic analysis of floating bridges.

Recently the NPRA has started several research projects regarding floating bridge structures as part of a ferry-free coastal route E39 between Kristiansand and Trondheim in Norway, where they aim to develop current methods of design.

In the present text a dynamic analysis in frequency domain will be given and theory on stochastic dynamic modelling of a floating bridge is described, including challenges regarding frequency-dependent hydrodynamic added mass and damping. Preliminary results will be given from a frequency domain analysis of the stresses on the pontoon.

Although a lot of research has gone in to the topic of floating bridges, the focus point has mostly been on the structural response in terms of displacement, velocity and acceleration of structural points and as far as the author is aware, not much literature on local stress distributions for floating pontoon bridges is published. This paper aims to shed some light on general stochastic design as well as local stress distribution.

2 System Modelling

The linear stochastic dynamic response of a floating bridge structure can be described using the equation of motion to capture the dynamics of the structure, potential theory to find the hydrodynamic added mass and damping and the wave excitation force from the fluid-structure interaction and stochastic theory to implement the randomness of the wave excitation force.

2.1 Equation of Motion

The equation of motion describing the linear dynamic behaviour of the floating bridge is described in time domain as shown in (1) .

$$[M_s]\{\ddot{u}(t)\} + [C_s]\{\dot{u}(t)\} + [K_s]\{u(t)\} = \{q_h(t)\} \quad (1)$$

Here, $[M_s]$, $[C_s]$ and $[K_s]$ are the frequency independent structural mass-, damping- and stiffness matrices. The vector notation $\{u\}$ is the structural response and the dots above represents derivatives of time t. The vector $\{q_h(t)\}$ represents the hydrostatic and hydrodynamic load vector.

2.1.1 Frequency Domain Representation

For a single harmonic small amplitude wave, $\{q_h(t)\}$ can be described as a harmonic wave proportional to $e^{i\omega t}$ as shown in (2).

As an extra step in the equation, the derivatives of the structural response are derived and collected within the parenthesis.

$$\{q_h(t)\} = -\left(-\omega^2[M_h(\omega)] + i\omega[C_h(\omega)] + [K_h]\right) \cdot\{Z_u(\omega)\}e^{i\omega t} + \{Z_q(\omega)\}e^{i\omega t} \quad (2)$$

Here, $[M_h(\omega)]$ and $[C_h(\omega)]$ are the frequency dependent hydrodynamic added mass and damping and ω is the angular frequency. $[K_h]$ is the restoring stiffness assumed frequency independent for small amplitude motion. $\{Z_u(\omega)\}$ and $\{Z_q(\omega)\}$ are the complex structural response amplitude and the complex wave excitation force amplitude, respectively, and i is the imaginary unit. Substituting the expression for the hydrodynamic action given in (2) into the equation

of motion in (1) and rearranging the terms gives the frequency domain representation of the equation of motion.

$$\{Z_q(\omega)\} = \left[-\omega^2[M(\omega)] + i\omega[C(\omega)] + [K]\right] \cdot\{Z_u(\omega)\} \quad (3)$$

The inertia, damping and restoring matrices include the structural terms as well as the added hydrodynamic mass and damping. The combined system matrices are hence given as.

$$[M(\omega)] = [M_s] + [M_h(\omega)] \quad (4)$$

$$[C(\omega)] = [C_s] + [C_h(\omega)] \quad (5)$$

$$[K] = [K_s] + [K_h] \quad (6)$$

The response induced by a single harmonic wave is then obtained by rearranging the terms in (3) and introducing the frequency transfer function $[H(\omega)]$.

$$\{Z_u(\omega)\} = [H(\omega)]\{Z_q(\omega)\} \quad (7)$$

$$[H(\omega)] = \left[-\omega^2[M(\omega)] + i\omega[C(\omega)] + [K]\right]^{-1} \quad (8)$$

By use of the principle of superposition, it is possible within the framework of linear theory to incorporate a generalized description of the excitation represented as the sum of a finite number of harmonic waves. In case of a random sea state the excitation in frequency domain can be obtain by Fourier transform of the excitation time series.

2.1.2 Time Domain Representation

Assuming frequency independent restoring and causality the wave excitation force can be described in the time domain as shown in (9) by use of the convolution integral.

$$\{q_h(t)\} = \{q(t)\} - \int_{-\infty}^{\infty}[m_h(t-\tau)]\{\ddot{u}(t)\}d\tau - \int_{-\infty}^{\infty}[c_h(t-\tau)]\{\dot{u}(t)\}d\tau - [K_h]\{u(t)\} \quad (9)$$

Here, τ is time lag and $[m_h]$ and $[c_h]$ are the time domain representations of the hydrodynamic added mass and damping found from Fourier transform.

$$[m_h(t)] = \frac{1}{2\pi}\int_{-\infty}^{\infty}[M_h(\omega)]e^{i\omega t}d\omega \quad (10)$$

$$[c_h(t)] = \frac{1}{2\pi}\int_{-\infty}^{\infty}[C_h(\omega)]e^{i\omega t}d\omega \quad (11)$$

Using the impulse response function, $h(\cdot)$, the response can be obtained in time domain as a finite sum of system responses from hydrodynamic action impulses at different time steps.

$$\{u(t)\} = \int_{-\infty}^{\infty}[h(t-\tau)]\{q_h(\tau)\}d\tau \quad (12)$$

The impulse response function is found from Fourier transform of the frequency transfer function in (8).

$$[h(t)] = \frac{1}{2\pi}\int_{-\infty}^{\infty}[H(\omega)]e^{i\omega t}d\omega \quad (13)$$

Several methods exist to solve (9) in time domain. Such approaches are useful if non-linear behaviour is of interest.

2.2 Description of Sea Waves

For engineering purpose, the wind-generated waves are approximated as a locally stationary and homogeneous random field and the sea surface elevation $\eta(\{x\},t)$ becomes a function of time and the two-dimensional space vector for the horizontal surface at the mean water level.

$$\eta(\{x\},t) = \int_{-\infty}^{\infty} e^{i(\{\kappa\}\{x\}-\omega t)}dZ_\eta(\{\kappa\},\omega) \quad (14)$$

Here, $Z_\eta(\{\kappa\},\omega)$ is the spectral process of the sea surface elevation and $\{\kappa\} = \{\kappa_x, \kappa_y\}$ is the two-dimensional wave number vector.

The spectral process is, given the assumptions of stationarity and homogeneity, related to wave spectral density $S_{\eta_r\eta_s}(\{\kappa\},\omega)$ as described in (15).

$$E\left[dZ_{\eta_r}(\{\kappa\},\omega)dZ^{T*}_{\eta_s}(\{\kappa\},\omega)\right] = S_{\eta_r\eta_s}(\{\kappa\},\omega)d\kappa_x d\kappa_y d\omega \quad (15)$$

Here, the subscripts r and s refer to points in time and space. The superscripts T and $*$ refer to the mathematical operations transpose and complex conjugate, respectively. The operation $E[\cdot]$ is the expected value.

The wave spectral density is divided into a cross-spectral term with $r \neq s$ and auto-spectral terms with $r = s$. The auto-spectral density is denoted $S_\eta(\omega,\theta)$.

The wave number vector can be described as a function of the wave direction θ and the modulus κ.

$$\{\kappa\} = \begin{Bmatrix}\cos\theta \\ \sin\theta\end{Bmatrix}\kappa \quad (16)$$

Furthermore, within the first-order Stokes theory κ and ω are related through the dispersion relationship given in (17).

$$\omega^2 = g\kappa\tanh(\kappa h) \quad (17)$$

Here, g is the gravitational acceleration and h is the water depth. In the special case of deep water waves the dispersion relationship can be approximated as $\omega^2 \approx g\kappa$. As a result of this approximation the spectral density can be described as a function of wave direction and frequency.

The auto-spectral density is generally a function of the frequency-dependent directional distribution $D(\omega,\theta)$ and the one-dimensional wave spectral density $S_\eta(\omega)$. For simplicity, the directional distribution is normally assumed to be frequency-independent as given in (18).

$$S_\eta(\omega,\theta) = S_\eta(\omega)D(\theta) \quad (18)$$

Due to the coherency, $Coh_{\eta_r\eta_s}(\omega)$, between point r and s the expression for the cross-spectral density given in (19) is a bit more complicated and is formulated by assuming deep water waves.

$$S_{\eta_r\eta_s}(\omega,\theta) = S_{\eta_r\eta_s}(\omega)Coh_{\eta_r\eta_s}(\omega)$$
$$Coh_{\eta_r\eta_s}(\omega) = \int_{-\pi}^{\pi} D(\theta)e^{-i\frac{|\omega|\kappa(\omega)}{g}(\Delta x\cos\theta+\Delta y\sin\theta)}d\theta \quad (19)$$

Here, Δx and Δy are the horizontal distances between point r and s.

2.2.1 Directional distribution

The directional distribution is commonly characterised by a bell shaped function centered around the mean wave direction. The simplest and one of the most commonly applied functional forms is the so-called cos-2s distribution, given in (20) for a specific mean wave direction.

$$D(\theta) = \frac{2^{2s-1}}{\pi}\frac{\Gamma^2(s+1)}{\Gamma(2s+1)}\cos^{2s}\left(\frac{\theta-\theta_m}{2}\right) \quad (20)$$
$$\pi \le (\theta-\theta_m) \le \pi$$

Here, s is the spreading parameter, $\Gamma(\cdot)$ is the Gamma function and θ_m is the mean wave direction.

2.3 Fluid structure interaction

The current analysis of floating bridges is based on the assumption of water being incompressible, non-viscous and irrotational. Then, within the framework of potential theory, the flow field is governed by Laplace's equation, given in (21) for Cartesian coordinates [8].

$$\nabla^2\Phi = \frac{\partial^2\Phi}{\partial x^2}+\frac{\partial^2\Phi}{\partial y^2}+\frac{\partial^2\Phi}{\partial z^2} = 0 \quad (21)$$

Here, Φ is the velocity potential and x, y and z are Cartesian coordinates. Hence, the basic problem at hand is to find the solution of the Laplace's equation in terms of the velocity potential.

Assuming no current and by virtue of the principle of superposition the velocity potential can be obtained from the linear problem given in (22).

$$\Phi = \underbrace{\varphi_0 e^{-i\omega t} + \varphi_7 e^{-i\omega t}}_{\text{diffraction problem}} + \underbrace{\sum_{k=1}^{6} \phi_k \dot{u}_k}_{\text{radiation problem}} \tag{22}$$

Here, φ_0 and φ_7 represents the velocity potential from the incident- and diffracted waves, respectively. ϕ_k represents the velocity potential per unit velocity from radiated waves and $\dot{u}_k$ represents the time derivative of the complex motion of the body in the water and together they represent the velocity potential from radiated waves $\varphi_k = \phi_k \dot{u}_k$ when the body is oscillating in the k'th degree of freedom.

From first-order Stokes theory the velocity potential for the incident wave is known. To obtain a physical legitimate solution for the other seven velocity potentials in (22) the Laplace's equation in (21) must be satisfied together with the free-surface boundary condition at the mean water level, the kinematic boundary conditions at the seabed and on the wetted body surface and the radiation condition. Using the indirect boundary integral formulation and applying Green's second identity it is possible to obtain solutions for each of the seven velocity potentials and the pressure p can then be obtained through Bernoulli's equation. Applying specific velocity potentials in Bernoulli's equation and integrating the hydrodynamic pressure over the wetted body surface it is possible to obtain expressions for the wave excitation force and the hydrodynamic added mass and damping when comparing to the equation for steady-state harmonic rigid body motion is given in (23).

$$q_j e^{-i\omega t} = \sum_{k=1}^{6} \left(M_{jk}(\omega) \ddot{u}_k + C_{jk}(\omega) \dot{u}_k + K_{jk} u_k \right) \tag{23}$$

Here, the index notations of (4), (5) and (6) is applied.

2.3.1 Wave Excitation Load

The diffraction problem describes the scenario of a fixed body in incident waves. By only including φ_0 and φ_7 in Bernoulli's equation it is possible to obtain the hydrodynamic action by integrating the hydrodynamic pressure over the wetted body surface S_0.

$$q_j = -i\omega\rho \int_{S_0} (\varphi_0 + \varphi_7) n_k \, dS \tag{24}$$

Here, n_k represents the component of the surface normal vector in the direction of the k'th degree of freedom. Comparing the expression with (23) the force is identified as the wave excitation force.

2.3.2 Hydrodynamic Added Mass and Damping

The radiation problem describes the scenario of a body oscillating in calm sea. Using the same approach as described in section 2.3.1 the hydrodynamic action from a body oscillating in calm water can be found.

$$\begin{aligned} q_j &= -i\omega\rho \dot{u}_j \int_{S_0} \phi_j n_k \, dS \\ &= \underbrace{\rho \, \mathrm{Re}\left(\int_{S_0} \phi_j n_k \, dS \right)}_{M_{h,jk}(\omega)} \ddot{u}_j + \underbrace{\rho\omega \, \mathrm{Im}\left(\int_{S_0} \phi_j n_k \, dS \right)}_{C_{h,jk}(\omega)} \dot{u}_j \end{aligned} \tag{25}$$

Comparing the expression with (23) the hydrodynamic added mass and damping can be identified.

3 Solution Strategy

It is commonly assumed, within the field of civil engineering structural dynamics, that structural damping is very small and hence can be neglected when calculating the natural frequencies and natural modes of a classically damped system. In the case of fluid structure interaction there is a significant contribution to the damping from the hydrodynamic damping $[C_h(\omega)]$ and so the system instead is categorised as a non-classically damped system. Procedures exists to calculate this higher order eigenvalue problem by use of the state-space approach [9]. The solution consists of complex eigenvalues and complex eigenvectors.

In the context of this article, the dynamic response is calculated using the direct frequency response method with the structure subjected to a set of unit amplitude wave with periods ranging from 1 second to 15 seconds.

3.1 Direct Frequency Response Method

The frequency domain representation described in section 2.1.1 applies the complex frequency transfer function $[H(\omega)]$ given in (8) to obtain solutions in the frequency domain. The response amplitude $\{Z_u(\omega)\}$ is a complex quantity describing the amplitude and the phase angle of the dynamic response.

By splitting the load into a real part $\{Z_{q,\mathrm{Re}}(\omega)\}$ and an imaginary part $\{Z_{q,\mathrm{Im}}(\omega)\}$ as described in [10] the solution can be as shown in (26).

$$\{Z_u(\omega)\} = [H(\omega)]\{Z_{q,\mathrm{Re}}(\omega)\} + i[H(\omega)]\{Z_{q,\mathrm{Im}}(\omega)\} \quad (26)$$

4 Case Study

4.1 Description of Floating Bridge Model

The model is a simplified floating pontoon bridge with pontoon dimensions equal to the pontoons used in the mid sections of the Bergsøysund Bridge (Norway).

The model consists of two horizontal beams, one vertical beam and a pontoon. The dimensions of the bridge are illustrated in Figure 1 where the x-, y- and z-axis corresponds to surge, sway and heave, respectfully.

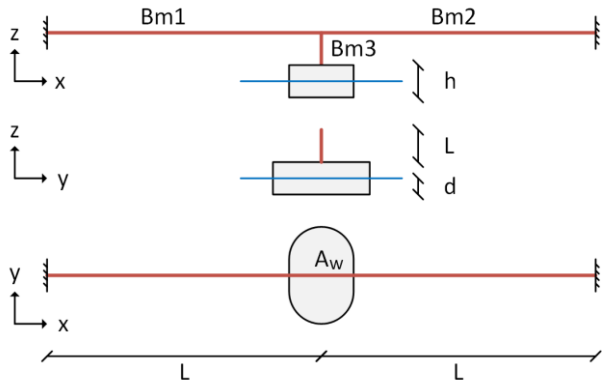

Figure 1. Bridge schematics

The cross-sectional properties of the beam elements are given in Table 1.

Table 1. Beam element properties

	L [m]	I_{xx} [m^4]	I_{yy} [m^4]	I_{zz} [m^4]
Bm1	400	1.07E-04	2.65E+00	9.21E-01
Bm2	400	1.07E-04	2.65E+00	9.21E-01
Bm3	8.02	1.17E+01	5.86E+00	5.86E+00

The mass properties and dimensions of the pontoon are listed in Table 2 and Table 3, respectively.

Table 2. Pontoon mass properties

M [kg]	r_{xx} [m^2]	r_{yy} [m^2]	r_{zz} [m^2]
1.37E+06	1.01E+01	6..80E+00	1.15E+01

The symbols I_{jj} and r_{jj} represents the second moment of area and the radius of gyration around the j'th axis, respectively. I_{xx} is the torsional moment of inertia.

Table 3. Pontoon dimensions with final draft

h [m]	d [m]	A_w [m^2]
6.98	3.61	594

Supports are located at each end of the floating bridge model and modelled as fixed in all degrees of freedom.

4.2 Numerical analysis

Due to the hydrodynamic added mass and damping, it is crucial to know the correct pontoon draft before commencing the dynamic analysis. Therefore, a static analysis is first carried out.

4.2.1 Static Equilibrium

From equilibrium between the pontoon mass and buoyancy from the displaced water, the initial draft of the pontoon is found. The static analysis is then carried out by replacing the pontoon with a vertical spring stiffness from the waterplane area and the water density. Applying gravitational loads to the static model the vertical displacement is computed. The final draft d is found by combining

the result from the static analysis with the initial draft.

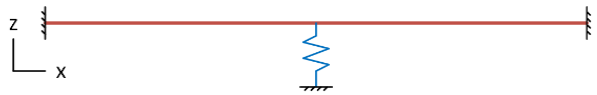

Figure 2. Static model with pontoon spring and gravitational load

4.2.2 Environmental Load Modelling

The hydrodynamic restoring, added mass and damping is calculated using a boundary element method software. A panel model of the pontoon surface as the one in Figure 3 is created and given as input to the software. The panel model used consists of 632 panel elements and is subjected to 60 unit amplitude waves with periods $T = \{1 : 0.25 : 15\}$ seconds each with a wave direction of 90 degrees from the global x-axis corresponding to sway. The water depth is set equal to 1000 meters.

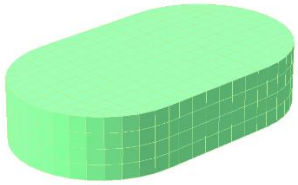

Figure 3. Panel- and structural model of pontoon

The mesh size of the panel model is roughly 2 meters, which according to [11] requires a minimum wavelength of 16 meters or in this case an equivalent wave period of approximately 3.2 seconds.

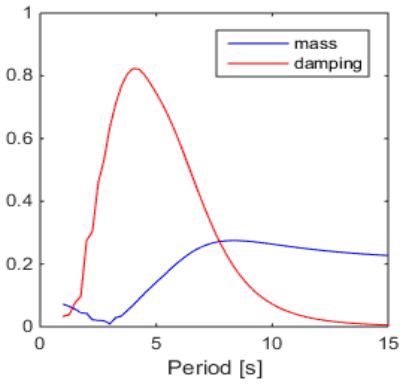

Figure 4. Normalized hydrodynamic added mass and damping in y-direction (sway). Normalization factors are $f_m = 2.19\text{E}{+}06$ and $f_c = 6.87\text{E}{+}05$ for added mass and damping, respectively

From the analysis, information of the hydrodynamic added mass and damping as a function of the period is illustrated in Figure 4.

4.2.3 Applied Rayleigh Damping

Assuming a damping ratio of $\zeta = 0.02$ the Rayleigh damping is calibrated using the first two horizontal undamped natural periods $T_{n1} = 44.5\text{s}$ and $T_{n2} = 13.9\text{s}$ found from solving the classical eigenvalue problem. From the sway response of the midpoint of the floating bridge, it can be checked whether or not appropriate structural damping is applied. It is important to have a sufficiently low mass proportional damping in order not to damp out the wave response.

5 Results

From the dynamic analysis carried out in the frequency domain it is possible to obtain some preliminary results of the stress distribution in the pontoon. The stress response from a set of 60 unit amplitude mono-chromatic beam sea waves have been analysed and specific characteristics of the frequency distribution of von Mises stress has been observed. At high frequency waves (period in the range of 1 second to 5 seconds) the largest stresses in the pontoon are located in the front part of the pontoon and on the corners connecting the front vertical concrete plates to the top- and bottom concrete plates, see Figure 5. Maximum values are in the range of 0.97 MPa.

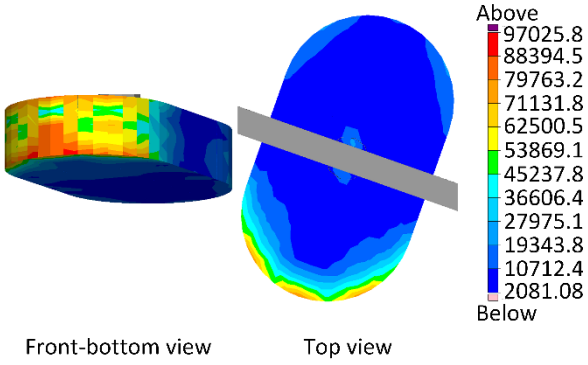

Figure 5. Von Mises stress on pontoon for monochromatic wave excitation force with $T = 2.25\text{s}$. The unit is Pa

At lower frequencies the largest von Mises stress is located exclusively around the connection point

between the pontoon and the vertical beam as illustrated in Figure 6. The stresses are in this case as high as 33.8 MPa.

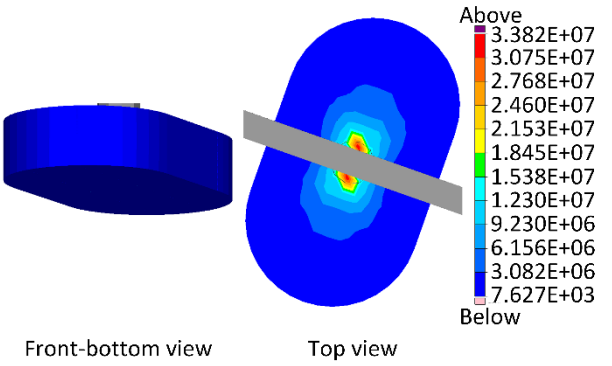

Figure 6. Von Mises stress on pontoon for monochromatic wave excitation force with $T = 8.50\text{s}$ *. The unit is Pa*

The minimum stresses at the low frequency wave excitation is roughly the same order as the stresses from the high frequency wave excitation force. It is believed that the high stress is a result of the high wave loads on the pontoon under long waves.

6 Conclusion and further work

The paper has presented general theory on solutions of the equation of motion in both time- and frequency domain and has explained how to incorporate the randomness of the sea state into the design using stochastic theory. Also a brief discussion of how potential theory and boundary element methods can be used when dealing with a non-classically damped system such as a floating bridge structure.

A case study of a simplified floating bridge structure has been presented and preliminary results of the stress distribution on the pontoon is shown.

From the preliminary analysis in frequency domain it can be concluded from the results given in Figure 5 and Figure 6 that the joint between the pontoon and the beam bridge structure is crucial in the design of the pontoon and, if not thoughtfully carried out, can generate high stresses in the pontoon surface elements.

Although the simplified pontoon bridge is made to resemble a realistic floating bridge structure, many details are lost in the simplification, such as a proper connection between pontoon and bridge deck. Future work includes more pontoons and a stochastic dynamic analysis in frequency- and time domain.

7 Acknowledgement

The late Prof. Ragnar Sigbjörnsson has contributed to sections 1, 2.1 and 2.2 with an initial draft.

8 References

[1] Skorpa L. Developing new methods to cross wide and deep Norwegian fjords. Procedia Engineeering. 2010; 4(1877): p. 81-89.

[2] Holand I,LI. Salhus floating bridge: theory and hydrodynamic coefficients. SINTEF Report. Trondheim: SINTEF; 1972.

[3] Sigbjörnsson R. LI. Wave-induced Vibrations of a Floating Bridge: The Salhus Bridge. Trondheim: SINTEF; 1975.

[4] Sigbjörnsson R,LI. Wave-induced Vibrations of a Floating Bridge: A Monte Carlo Approach. SINTEF; 1975.

[5] Holand I,I,SR. Dynamic analysis of a curved floating bridge. In IABSE Proceedings; 1977. p. P-5/77.

[6] Langen I,SR. On stochastic dynamics of floating bridges. Eng. Struct. 1980 October; 2.

[7] Langen I. Frequency Domain Analysis of a Floating Bridge Exposed to Irregular Short-crested Waves. Trondheim: SINTEF; 1980.

[8] Munson BR, Young DF, Okiishi TH, Huebsch WW. Fundamentals of Fluid Mechanics. 6th ed.: John Wiley & Sons; 2010.

[9] He, J., Fu, Z. Modal Analysis: Butterworth-Heinemann; 2001.

[10] DNV-GL. Sesam User Manual, Sestra, Valid from program version 8.6. 2014 October 31..

[11] Faltinsen OM. Sea Loads on Ships and Offshore Structures: Cambridge University Press; 1990.